Visible to vacuum ultraviolet dielectric functions of epitaxial graphene on 3C and 4H SiC polytypes determined by spectroscopic ellipsometry

A. Boosalis, T. Hofmann, Vanya Darakchieva, Rositsa Yakimova and M. Schubert

Original Publication:

A. Boosalis, T. Hofmann, Vanya Darakchieva, Rositsa Yakimova and M. Schubert, Visible to vacuum ultraviolet dielectric functions of epitaxial graphene on 3C and 4H SiC polytypes determined by spectroscopic ellipsometry, 2012, Applied Physics Letters, (101), 1, 011912.
http://dx.doi.org/10.1063/1.4732159

AIP | Applied Physics Letters

Visible to vacuum ultraviolet dielectric functions of epitaxial graphene on 3C and 4H SiC polytypes determined by spectroscopic ellipsometry

A. Boosalis, T. Hofmann, V. Darakchieva, R. Yakimova, and M. Schubert

Citation: Appl. Phys. Lett. **101**, 011912 (2012); doi: 10.1063/1.4732159
View online: http://dx.doi.org/10.1063/1.4732159
View Table of Contents: http://apl.aip.org/resource/1/APPLAB/v101/i1
Published by the American Institute of Physics.

Related Articles

Spin-dependent transport through a quantum wire on a graphene surface
Appl. Phys. Lett. 102, 011911 (2013)

Magnetoresistance and shot noise in graphene-based nanostructure with effective exchange field
J. Appl. Phys. 112, 123719 (2012)

Markovian dissipative coarse grained molecular dynamics for a simple 2D graphene model
J. Chem. Phys. 137, 234103 (2012)

Preferred armchair edges of epitaxial graphene on 6H-SiC(0001) by thermal decomposition
Appl. Phys. Lett. 101, 241903 (2012)

Communication: Oscillated band gaps of B/N-codoped α-graphyne
J. Chem. Phys. 137, 201101 (2012)

Additional information on Appl. Phys. Lett.

Journal Homepage: http://apl.aip.org/
Journal Information: http://apl.aip.org/about/about_the_journal
Top downloads: http://apl.aip.org/features/most_downloaded
Information for Authors: http://apl.aip.org/authors

ADVERTISEMENT

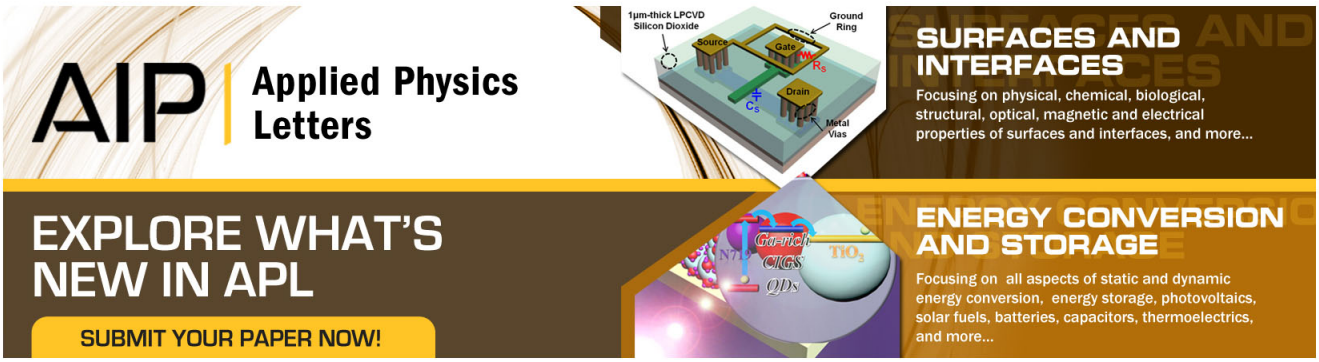

Visible to vacuum ultraviolet dielectric functions of epitaxial graphene on 3C and 4H SiC polytypes determined by spectroscopic ellipsometry

A. Boosalis,[1] T. Hofmann,[1] V. Darakchieva,[2] R. Yakimova,[2] and M. Schubert[1]
[1]*Department of Electrical Engineering and Nebraska Center for Materials and Nanoscience, University of Nebraska-Lincoln, Lincoln, Nebraska 68588-0511, USA*
[2]*Department of Physics, Chemistry, and Biology (IFM), Linköping University, SE 581 83 Linköping, Sweden*

(Received 16 April 2012; accepted 12 June 2012; published online 6 July 2012)

Spectroscopic ellipsometry measurements in the visible to vacuum-ultraviolet spectra (3.5–9.5 eV) are performed to determine the dielectric function of epitaxial graphene on SiC polytypes, including 4H (C-face and Si-face) and 3C SiC (Si-face). The model dielectric function of graphene is composed of two harmonic oscillators and allows the determination of graphene quality, morphology, and strain. A characteristic van Hove singularity at 4.5 eV is present in the dielectric function of all samples, in agreement with observations on exfoliated as well as chemical vapor deposited graphene in the visible range. Model dielectric function analysis suggests that none of our graphene layers experience a significant degree of strain. Graphene grown on the Si-face of 4H SiC exhibits a dielectric function most similar to theoretical predictions for graphene. The carbon buffer layer common for graphene on Si-faces is found to increase polarizability of graphene in the investigated spectrum. © *2012 American Institute of Physics*. [http://dx.doi.org/10.1063/1.4732159]

As silicon reaches its scaling limits,[1] the search for a replacement semiconductor material has focused recent attention on graphene. Research has shown graphene to exhibit superior electronic properties.[2,3] Refinement of deposition techniques for epitaxial graphene onto large scale substrates, such as by thermal sublimation of silicon carbide, may offer the realization of high performance electronic devices. In order to harness graphene for commercial use, further development of epitaxial growth processes must continue, and a better understanding of the electronic and structural relationships in epitaxial graphene must be reached.[4,5] Currently, there is only a limited understanding of the influence of the substrate on the electrical properties of epitaxial graphene. Growth of epitaxial graphene on different polytypes of silicon carbide may provide insight into the various interactions between the substrate and graphene. Graphene growth on 4H and 6H SiC was reported on numerous occasions,[6–10] and it was obtained that both structural and electronic properties of graphene layers differ drastically. The dielectric function spectra contain unique fingerprints of the electronic properties of semiconductor materials and are suitable for characterization of electronic band structure parameters.[11] Likewise, these functions can be used for monitoring structure-related properties such as strain, as well as for quality control during production.

Presently, knowledge on the dielectric functions of epitaxial graphene grown on various substrates is not exhaustive. Theoretical calculations predict a van Hove singularity within the 2-dimensional Brilloiun zone along the 6-fold degenerate directions between symmetry points K and K'.[12] This singularity can be associated with the characteristic critical-point (CP) feature observed in dielectric function spectra of exfoliated graphene[13,14] and graphene grown by chemical vapor deposition for photon energies around 4.5 eV.[15]

In this work, we report dielectric function spectra for epitaxial graphene layers grown by thermal sublimation on 3C, 4H silicon-face, and 4H carbon-face silicon carbide from the visible light region to the ultra-violet (3.5–9.5 eV). The dielectric function spectra are obtained from spectroscopic ellipsometry measurements and subsequent model dielectric function (MDF) analysis. We employ traditional physical model lineshape analysis procedures and provide quantitative model parameters for the band-to-band transition characteristics of graphene in the ultra violet region. We observe that these parameters vary between the different polytypes and discuss possible origins.

The samples investigated here were formed by high temperature sublimation epitaxy[16] of silicon on the Si (0001) and C $(000\bar{1})$ terminated faces of a 4H SiC substrate (4H-Si and 4H-C). Similarly, epitaxial graphene was formed on a thick epitaxial 3C SiC layer, with the 3C SiC layer grown on the Si face of a 6H SiC substrate.[17] This 3C sample has a (111) orientation and is Si terminated (3C-Si). Samples were stored in normal ambient after growth and not treated further. Ellispometry measurements were carried out on the 4H-Si, 4H-C, and 3C-Si samples before and after epitaxial graphene growth. Bare 3C and 4H substrates were measured to determine the dielectric response of the silicon carbide polytypes without graphene. All measurements were performed upon reflection of the sample, on a J.A. Woollam VUV-302 VASE ellipsometer in a nitrogen-purged environment. Measurements were performed for photon energies from 3.5 to 9.5 eV, with spectral increments of 0.05 eV, at 50°, 60°, and 70° angle of incidence.

Ellipsometry determines the ratio ρ of the complex-valued Fresnel reflection coefficients r_p and r_s for light polarized parallel p and perpendicular s to the plane of incidence, respectively, and is commonly presented by parameters Ψ and Δ, where $\rho = r_p/r_s = \tan\Psi e^{i\Delta}$.[18] Figure 1 depicts experimental and best-match model calculated Ψ and Δ spectra from all investigated graphene samples. The experimental data reveal large differences between the Si and C faces of the 4H SiC sample, whereas bare substrate measurements

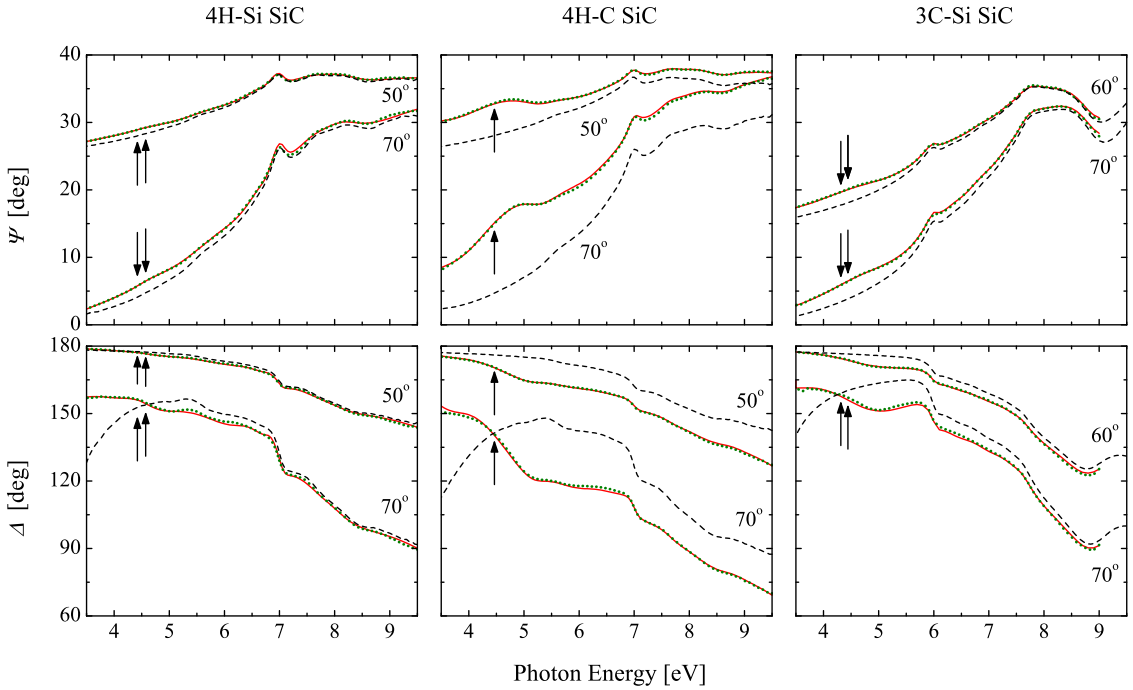

FIG. 1. Experimental (dotted lines; green) and best-match model calculated (solid lines; red) Ψ and Δ spectra for graphene grown on 4H and 3C SiC compared to bare SiC substrates (dashed lines; black) at incidence angles $\Phi_a = 50°$, $\Phi_a = 60°$, and $\Phi_a = 70°$. Vertical arrowed lines represent the best-match model oscillator energies for each polytype.

yielded matching Ψ spectra for both Si and C faces. The differences exhibited in Fig. 1 between the Si and C faces are due only to the expitaxial graphene properties, including thickness. While this influence is seen most strikingly at the CP peak caused by the van Hove singularity, occurring here at photon energies around 4.5 eV, graphene influences the entire spectroscopic response from 3.5 to 9.5 eV. Note that the 3C spectra in Fig. 1 are limited due to lack of reflected light intensity above 9 eV.

A stratified layer optical model composed of a substrate, an interface layer between the substrate and the graphene, a graphene layer, and a roughness layer between the graphene and the air (see Fig. 2) is used here to analyze the ellipsometric data. All layers are treated isotropically in our model since ellipsometry has no sensitivity to the out-of-plane polarizability of ultra-thin layers.[19–21] Experimental Ψ and Δ spectra, obtained from bare 4H and 3C SiC substrates, were analyzed employing a sum of broadened harmonic oscillator lineshapes. The obtained MDF spectra are equivalent to those reported previously for 4H (Refs. 22 and 23) and 3C (Ref. 24) SiC, but are omitted here for brevity. The best-match substrate MDF parameters were then used in the analysis of the epitaxial graphene samples but were not further varied. The graphene MDF is composed of Lorentzian and Gaussian oscillators such that $\varepsilon = 1 + \varepsilon_L + \varepsilon_G$,[15]

$$\varepsilon_L(E) = \frac{A_L \gamma_L}{{E_L}^2 - E^2 - i\gamma_L E}, \quad (1)$$

$$\Im\{\varepsilon_G\}(E) = A_G\left[e^{-\left(\frac{E-E_G}{\sigma}\right)^2} + e^{-\left(\frac{E+E_G}{\sigma}\right)^2}\right],\ \sigma = \frac{\gamma_G}{2\sqrt{\ln(2)}}, \quad (2)$$

where $A_{L,G}$, $E_{L,G}$, and $\gamma_{L,G}$ denote the amplitude, the CP transition energies, and the broadening of the Lorentzian and Gaussian oscillators, respectively.

On 4H-Si and 3C-Si, the carbon buffer layer atoms are strongly bonded to the substrate and form a $(6\sqrt{3} \times 6\sqrt{3})R30°$ surface reconstruction,[25–27] while on 4H-C, there is no unique surface reconstruction.[28] In our optical model, the interface layer accounts for this buffer layer, and also the roughness of the substrate surface, an effect of the slight off-axis cut of the SiC substrate, and non-uniform sublimation of silicon from the SiC substrate. A linear effective medium approximation (EMA) comprised of 50% substrate and 50% graphene was used to create a suitable MDF for the combined effect of the buffer layer and surface roughness in

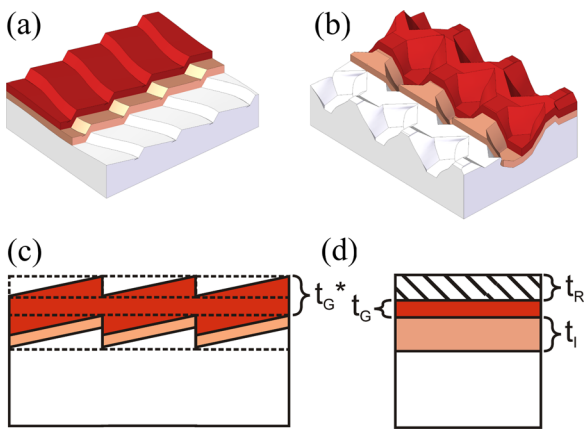

FIG. 2. (a) Illustration of typical graphene growth on the Si face of 4H SiC. White coloring represents the resulting SiC surface morphology after thermal treatment. Orange coloring represents the interface layer. Red coloring represents graphene. (b) Illustration of graphene growth on the C face of 4H SiC. (c) Illustration of graphene growth on an off-cut axis substrate. Solid lines represent the divisions between the graphene and the void, the graphene and buffer layer, and the buffer layer and the substrate. Dotted lines indicate the plane parallel layers assumed by the ellipsometer. The thickness t_G* is the true thickness of the graphene. (d) Illustration of the final optical model with effective ellipsometric thickness parameters t_R, t_G, and t_I.

a single interface layer. This is shown graphically in Fig. 2. The only varied parameter during the data analysis that was unique to the interface layer was its thickness (t_I). Likewise, a surface roughness layer modeled with another linear EMA comprised of 50% graphene and 50% ambient was implemented with a thickness t_R. During data analysis, the thicknesses of the surface roughness layer (t_R), epitaxial graphene layer (t_G), and the interface layer (t_I), and the graphene MDF parameters are varied until best-match between experimental and model calculated Ψ and Δ spectra is achieved. Best-match model parameters for each surface are presented in Table I. We note that the resulting graphene layer thickness for 4H-Si and 3C-Si are closer to the ideal graphene monolayer thickness than 4H-C, which forms multilayer graphene (Table I).

Figure 3 presents the imaginary part (ε_2) of the best-match MDF obtained here for graphene on 3C and 4H SiC in comparison with theoretical results obtained by Yang *et al.*[29] for graphene and graphite. The ε_2 spectra are dominated by the well known CP transition.[13–15] Comparing the CP peak energies[30] of graphene (4.53 eV) and graphite (4.37 eV) in Fig. 3 reveals that 4H-Si (4.51 eV) is closest to graphene. This conclusion is corroborated by the E_G and γ_G parameters, which run parallel with the CP peak energies and show agreement between the 3C-Si and 4H-C samples, while the 4H-Si sample shows a higher E_G and lower γ_G. Together these parameters show that while the carbon film on 3C-Si is thin (mono- or bi-layer), it has an electronic structure similar to graphite. This is attributed to the relatively high defect density on the as-grown 3C substrate, which leads to the formation of thick graphite-like islands during the sublimation (to be reported elsewhere). It is noteworthy that the 3C-Si sample exhibits the dielectric function of graphite and is far from that of amorphous carbon.[31] All of the samples studied here displayed only one CP peak energy between 3.5 and 9.5 eV, in contrast to predictions by Trevisanutto *et al.*[32] of an exitonic resonance between 8.3 and 9.6 eV. Similarly, Pellegrino, Angilella, and Pucci predict multiple CPs with shifting energies for graphene under strain, suggesting that none of the investigated samples have significant strain to alter the optical conductivity.[33]

Examination of Figs. 3(a) and 3(c) shows a heightened polarizability throughout the spectrum for the 4H-Si and 3C-Si samples in contrast to Fig. 3(b) for the 4H-C sample. This increased polarizability can be attributed to either the $(6\sqrt{3} \times 6\sqrt{3})$R30° surface reconstructed carbon buffer layer of the 4H-Si and 3C-Si samples or a charge transfer from the SiC substrate predicted by Varchon *et al.*[34] In order for doping to affect the MDF above 3.5 eV evenly, both the mobility and free charge carrier concentration must be extraordinarily large, which suggests the cause is linked to the unique surface reconstruction of the buffer layer.

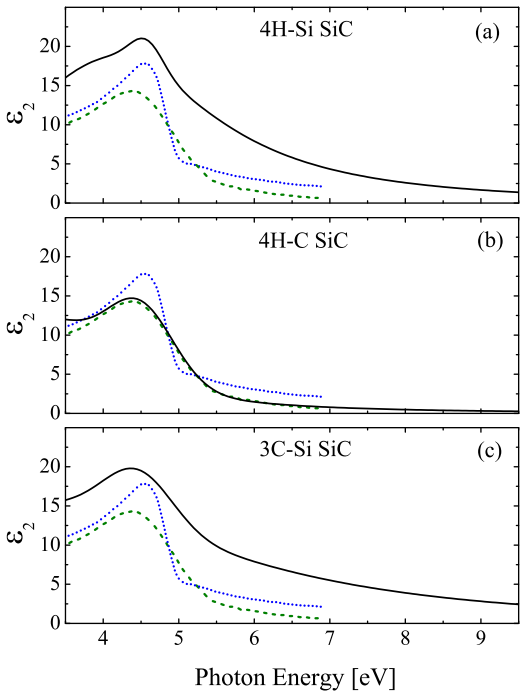

FIG. 3. Imaginary part of the dielectric function for epitaxial graphene relative to substrate polytype (solid lines; black) with theoretical graphene- (dotted lines; blue) and graphite-exciton (dashed lines; green) enhanced dielectric functions from Yang *et al.*[29]

TABLE I. Best-match model parameters of graphene on SiC substrates. The error limits given in parenthesis denote the uncertainty of the last significant digit (90% reliability). Film thicknesses are listed in physical order from ambient to substrate.

Parameter	3C-Si	4H-Si	4H-C
A_L	13(5)	18(1)	11.7(1)
E_L (eV)	4.3(3)	4.44(5)	3.37(2)
γ_L	6.2(5)	3.3(1)	2.17(5)
A_G	6(3)	3.5(5)	9.6(2)
E_G (eV)	4.46(5)	4.58(2)	4.486(6)
γ_G	1.1(1)	0.50(7)	1.06(2)
CP Peak (eV)	4.37	4.51	4.38
t_R (nm)	0.2(3)	0.09(5)	0.075(6)
t_G (nm)	0.1(2)	0.14(9)	2.04(3)
t_I (nm)	0.8(7)	0.4(1)	2.90(9)

The graphene thickness parameter for the 4H-Si and 3C-Si samples is smaller than the 0.35 nm value given by Varchon *et al.*[34] for monolayer graphene. This may be due to the fact that the actual surface morphology influenced by substrate defects and uneven Si sublimation, for instance, is not accounted for in the plane parallel layer model employed for the data analysis here. Surface morphology illustrations are presented in Figs. 2(a) and 2(c) as described in Ref. 35. Morphology considerations then also explain the large thickness of the interface layer (t_I) for 4H-C and 3C-Si, as the true graphene thickness is partially hidden in the ellipsometric interface thickness parameter t_I. An illustration of this is shown in Figs. 2(b) and 2(c).

In conclusion, spectroscopic ellipsometry measurements have been performed on epitaxial graphene grown on the 4H and 3C polytypes of SiC. The best-match MDFs for the graphene layer on each growth surface exhibited a CP peak which allowed comparison to theoretical predictions for the dielectric function of graphene and graphite, and determination of graphene quality, morphology, and strain. Epitaxial graphene grown on 4H-Si exhibited a MDF closest to that of theoretical graphene, while graphene grown on 3C-Si and 4H-C exhibited a MDF similar to graphite, despite a 3C-Si graphene thickness indicative of monolayer graphene. The

carbon buffer layer present on the 3C-Si and 4H-Si samples produces an increased polarizability throughout the visible to ultraviolet spectrum. None of the samples investigated exhibited multiple MDF CPs of graphene under strain.

The authors would like to acknowledge financial support from the Army Research Office (W911NF-09-C-0097), the National Science Foundation (MRSEC DMR-0820521, MRI DMR-0922937, DMR-0907475, ECCS-0846329, and EPS-1004094), the Swedish Research Council (2010-3848, 2011-4447), the Swedish Governmental Agency for Innovation Systems (VINNMER 2011-03486), the Department of Commerce–NIST (70NANB11H165), the University of Nebraska-Lincoln, and the J. A. Woollam Foundation.

[1]Y. Taur, Y.-J. Mii, D. J. Frank, H.-S. Wong, D. A. Buchanan, S. J. Wind, S. A. Rishton, G. A. Sai-Halasz, and E. J. Nowak, IBM J. Res. Dev. **39**, 245 (1995).
[2]K. I. Bolotin, K. J. Sikes, Z. Jiang, M. Klima, G. Fudenberg, J. Hone, P. Kim, and H. L. Stormer, Solid State Commun. **146**, 351 (2008).
[3]J. M. Dawlaty, S. Shivaraman, M. Chandrashekhar, F. Rana, and M. G. Spencer, Appl. Phys. Lett. **92**, 042116 (2008).
[4]D. K. Gaskill, G. G. Jernigan, P. M. Campbell, J. L. Tedesco, J. C. Culbertson, B. L. VanMil, R. L. Myers-Ward, C. R. Eddy, J. J. Moon, D. Curtis, M. Hu, D. Wong *et al.*, ECS Trans. **19**, 117 (2009).
[5]P. N. First, W. A. de Heer, T. Seyller, C. Berger, J. A. Stroscio, and J.-S. Moon, MRS Bull. **35**, 296 (2010).
[6]J. Hass, R. Feng, J. E. Millán-Otoya, X. Li, M. Sprinkle, P. N. First, W. A. de Heer, E. H. Conrad, and C. Berger, Phys. Rev. B **75**, 214109 (2007).
[7]W. A. de Heer, C. Berger, X. Wu, P. N. First, E. H. Conrad, X. Li, T. Li, M. Sprinkle, J. Hass, M. L. Sadowski, M. Potemski, and G. Martinez, Solid State Commun. **143**, 92 (2007).
[8]K. V. Emtsev, A. Bostwick, K. Horn, J. Jobst, G. L. Kellogg, L. Ley, J. L. McChesney, T. Ohta, S. A. Reshanov, J. Rohrl, E. Rotenberg, A. K. Schmid *et al.*, Nature Mater. **8**, 203 (2009).
[9]F. Hiebel, P. Mallet, F. Varchon, L. Magaud, and J.-Y. Veuillen, Phys. Rev. B **78**, 153412 (2008).
[10]C. Virojanadara, M. Syväjarvi, R. Yakimova, L. I. Johansson, A. A. Zakharov, and T. Balasubramanian, Phys. Rev. B **78**, 245403 (2008).
[11]P. Yu and M. Cardona, *Fundamentals of Semiconductors* (Springer, Berlin, 1999).
[12]T. Stauber, N. M. R. Peres, and A. K. Geim, Phys. Rev. B **78**, 085432 (2008).
[13]V. G. Kravets, A. N. Grigorenko, R. R. Nair, P. Blake, S. Anissimova, K. S. Novoselov, and A. K. Geim, Phys. Rev. B **81**, 155413 (2010).
[14]J. W. Weber, V. E. Calado, and M. C. M. van de Sanden, Appl. Phys. Lett. **97**, 091904 (2010).
[15]F. J. Nelson, V. K. Kamineni, T. Zhang, E. S. Comfort, J. U. Lee, and A. C. Diebold, Appl. Phys. Lett. **97**, 253110 (2010).
[16]R. Yakimova, C. Virojanadara, D. Gogova, M. Syvjrvi, D. Siche, K. Larsson, and L. I. Johansson, Mater. Sci. Forum **645**, 565 (2010).
[17]R. Vasiliauskas, M. Marinova, M. Syvjrvi, R. Liljedahl, G. Zoulis, J. Lorenzzi, G. Ferro, S. Juillaguet, J. Camassel, E. Polychroniadis, and R. Yakimova, J. Cryst. Growth **324**, 7 (2011).
[18]M. Schubert, *Infrared Ellipsometry on Semiconductor Layer Structures: Phonons, Plasmons, and Polaritons*, Springer Tracts in Modern Physics Vol. 209 (Springer, Berlin, 2004).
[19]Note that the optical axis of the opaque 4H SiC substrates is normal to the sample surface, and the optical response is treated isotropically here.
[20]*Handbook of Ellipsometry*, edited by H. Thompkins and E. A. Irene (William Andrew, Highland Mills, 2004).
[21]M. Schubert, B. Rheinländer, J. A. Woollam, B. Johs, and C. M. Herzinger, J. Opt. Soc. Am. A **13**, 875 (1996).
[22]S. Zollner, J. G. Chen, E. Duda, T. Wetteroth, S. R. Wilson, and J. N. Hilfiker, J. Appl. Phys. **85**, 8353 (1999).
[23]O. P. A. Lindquist, K. Jrrendahl, S. Peters, J. T. Zettler, C. Cobet, N. Esser, D. E. Aspnes, A. Henry, and N. V. Edwards, Appl. Phys. Lett. **78**, 2715 (2001).
[24]S. Logothetidis and J. Petalas, J. Appl. Phys. **80**, 1768 (1996).
[25]A. Charrier, A. Coati, T. Argunova, F. Thibaudau, Y. Garreau, R. Pinchaux, I. Forbeaux, J.-M. Debever, M. Sauvage-Simkin, and J.-M. Themlin, J. Appl. Phys. **92**, 2479 (2002).
[26]G. M. Rutter, N. P. Guisinger, J. N. Crain, E. A. A. Jarvis, M. D. Stiles, T. Li, P. N. First, and J. A. Stroscio, Phys. Rev. B **76**, 235416 (2007).
[27]A. Ouerghi, A. Kahouli, D. Lucot, M. Portail, L. Travers, J. Gierak, J. Penuelas, P. Jegou, A. Shukla, T. Chassagne, and M. Zielinski, Appl. Phys. Lett. **96**, 191910 (2010).
[28]J. Hass, F. Varchon, J. E. Millán-Otoya, M. Sprinkle, N. Sharma, W. A. de Heer, C. Berger, P. N. First, L. Magaud, and E. H. Conrad, Phys. Rev. Lett. **100**, 125504 (2008).
[29]L. Yang, J. Deslippe, C.-H. Park, M. L. Cohen, and S. G. Louie, Phys. Rev. Lett. **103**, 186802 (2009).
[30]The CP peak energies which are located between E_L and E_G were determined using the numerical derivative of the ε_2 spectra in Fig. 3.
[31]J. Wagner and P. Lautenschlager, J. Appl. Phys. **59**, 2044 (1986).
[32]P. E. Trevisanutto, M. Holzmann, M. Côté, and V. Olevano, Phys. Rev. B **81**, 121405 (2010).
[33]F. M. D. Pellegrino, G. G. N. Angilella, and R. Pucci, Phys. Rev. B **81**, 035411 (2010).
[34]F. Varchon, R. Feng, J. Hass, X. Li, B. N. Nguyen, C. Naud, P. Mallet, J.-Y. Veuillen, C. Berger, E. H. Conrad, and L. Magaud, Phys. Rev. Lett. **99**, 126805 (2007).
[35]B. L. VanMil, R. L. Myers-Ward, J. L. Tedesco, C. R. Eddy, Jr., G. G. Jernigan, J. C. Culbertson, P. M. Campbell, J. McCrate, S. Kitt, and D. K. Gaskill, Mater. Sci. Forum **615–617**, 211 (2009).